Dependence of the ocean-atmosphere partitioning of carbon on temperature and alkalinity

Citation: Omta, Anne Willem et al. "Dependence of the Ocean-Atmosphere Partitioning of Carbon on Temperature and Alkalinity." Global Biogeochemical Cycles 25, 1 (January 2011): GB1003 © 2011 American Geophysical Union

As Published: http://dx.doi.org/10.1029/2010GB003839

Publisher: American Geophysical Union (AGU)

Persistent URL: http://hdl.handle.net/1721.1/118312

Version: Final published version: final published article, as it appeared in a journal, conference proceedings, or other formally published context

Dependence of the ocean-atmosphere partitioning of carbon on temperature and alkalinity

Anne Willem Omta,[1] Stephanie Dutkiewicz,[1] and Michael J. Follows[1]

Received 2 April 2010; revised 16 August 2010; accepted 29 September 2010; published 12 January 2011.

[1] We develop and extend a theoretical framework to analyze the impacts of changes in temperature and alkalinity on the ocean-atmosphere carbon partitioning. When investigating the impact of temperature, we assume that there is no change in the global ocean alkalinity. This idealized situation is probably most relevant on intermediate timescales of hundreds to thousands of years. Our results show that atmospheric pCO_2 depends approximately exponentially on the average ocean temperature, since the chemical equilibria involved have an exponential (Arrhenius-type) dependence. The dependence of pCO_2 on alkalinity is more complicated, and our theory suggests several regimes. The current ocean-atmosphere system appears to have an exponential dependence of pCO_2 on global mean ocean alkalinity, but at slightly higher alkalinities, the dependence becomes a power law. We perform experiments with a numerical physical-biogeochemical model to test the validity of our analytical theory in a more complex, ocean-like system: in general, the numerical results support the analytical inferences.

Citation: Omta, A. W., S. Dutkiewicz, and M. J. Follows (2011), Dependence of the ocean-atmosphere partitioning of carbon on temperature and alkalinity, *Global Biogeochem. Cycles*, *25*, GB1003, doi:10.1029/2010GB003839.

1. Introduction

[2] Currently, the oceans take up about 30% of the anthropogenically emitted carbon [*Orr et al.*, 2001]. This percentage will most certainly decrease with the ongoing anthropogenic carbon emissions, because the buffering capacity of the oceans diminishes as the oceanic carbon concentration increases [*Goodwin et al.*, 2007; *Omta et al.*, 2010] and carbonate ions at the ocean surface are neutralized by reaction with (anthropogenic) carbon dioxide. In addition, the solubility of carbon dioxide in water decreases with increasing temperature [*Lee and Millero*, 1995; *McKinley et al.*, 2006; *Takahashi et al.*, 1993]. Hence, a positive feedback is expected: any global warming due to an increasing amount of carbon in the atmosphere leads to a lower oceanic carbon uptake which in turn increases the warming [*Plattner et al.*, 2001; *Friedlingstein et al.*, 2006]. To obtain insight into the (long-term) impact of this temperature feedback, we develop a framework to consider the relationship between temperature and the ocean-atmosphere partitioning of carbon. This is significant not only for the prediction of future carbon partitioning as ocean temperatures rise, but also to gain a deeper understanding of CO_2 variations in the geological past.

[3] Several earlier studies have focused on the impact on atmospheric pCO_2 of localized perturbations of the ocean temperature [*Bacastow*, 1996; *Broecker et al.*, 1999; *DeVries and Primeau*, 2009]. Such perturbations can affect atmospheric pCO_2 through impacts on both the carbon solubility and the air-sea disequilibrium of carbon [*Toggweiler et al.*, 2003]. *DeVries and Primeau* [2009] have shown that the impact of the disequilibrium component scales with the strength of the overturning circulation. And, using their Green-function analysis, it can also be shown that the impact of the solubility component on atmospheric pCO_2 approximately scales with the average temperature of the ocean. Here, we instead consider the relation between the mean temperature of the whole ocean and atmospheric pCO_2. That is, we study the solubility component in isolation and we do not consider changes in the carbon disequilibrium.

[4] We assume that carbon has equilibrated between the atmosphere and the ocean, but that total global ocean alkalinity remains constant. This idealized situation is probably most relevant on intermediate timescales of thousands of years [*Archer et al.*, 1997]. Further assumptions are that the biological activity does not change and that total carbon in the system is constant.

[5] First, we derive a relationship between the ocean average temperature and atmospheric pCO_2 (throughout this article, "pCO_2" refers to the volume fraction of CO_2 in the atmosphere in ppmv), and show that it accurately predicts the results of three-dimensional physical/biogeochemical model simulations. We then compare specific predictions from our theoretical framework with observations from

[1]Department of Earth, Atmospheric and Planetary Sciences, Massachusetts Institute of Technology, Cambridge, Massachusetts, USA.

0886-6236/11/2010GB003839

Table 1. Variable Parameters Used in the Calculations With Value Ranges Between 0°C and 30°C[a]

Parameter	Units	Value Range	Definition	Interpretation
O	-	1.2–1.6	$-\frac{\partial \ln(K \times pCO_2)}{\partial \ln([CO_3^{2-}])}$	CO_3^{2-} scaling parameter
H	-	1.1–1.3	$\frac{\partial \ln(K \times pCO_2)}{\partial \ln[H^+]}$	H^+ scaling parameter
K	mol L^{-1} atm^{-1}	30–130	$\frac{[HCO_3^-]^2}{pCO_2 \times [CO_3^{2-}]}$	Equilibrium constant
K_H	L atm/mol	16–40	$\frac{pCO_2}{[CO_2]}$	Henry's law constant
a	$°C^{-1}$	0.041–0.052	$-\frac{\partial \ln K}{\partial T}$	Temperature dependence K
b	$°C^{-1}$	0.023–0.039	$\frac{\partial \ln K_H}{\partial T}$	Temperature dependence K_H

[a]From *Mehrbach et al.* [1973] and *Millero* [1995].

Takahashi et al. [1993] and *Key et al.* [2004]. Finally, we derive an expression for the dependence of the atmospheric CO_2 content on (carbonate) alkalinity.

2. Analysis

[6] Carbon in the ocean exists as multiple species: aqueous carbon dioxide (CO_2), carbonic acid (H_2CO_3), the bicarbonate ion (HCO_3^-), and the carbonate ion (CO_3^{2-}). The sum of all these compounds is called dissolved inorganic carbon (DIC) which we will denote as C:

$$C \equiv [CO_2] + [H_2CO_3] + [HCO_3^-] + [CO_3^{2-}] \quad (1)$$

The ocean has a high buffering capacity for CO_2, as it reacts with bases such as CO_3^{2-} to form HCO_3^-. A measure for this buffering capacity is given by the total titration alkalinity [*Chester*, 2000] which is the sum of the concentrations of all the conjugate bases of weak acids. In the ocean, HCO_3^- and CO_3^{2-} account for 95% of the total titration alkalinity [*Zeebe and Wolf-Gladrow*, 2001]. We will neglect other bases and approximate the total titration alkalinity by the carbonate alkalinity (which we will call A):

$$A \equiv [HCO_3^-] + 2 \times [CO_3^{2-}]. \quad (2)$$

[7] For all values of C and A, the relationship between atmospheric pCO_2, $[HCO_3^-]$, and $[CO_3^{2-}]$ is given by [*Broecker and Peng*, 1982]:

$$pCO_2 = \frac{[HCO_3^-]^2}{K \times [CO_3^{2-}]} \quad (3)$$

In this equation, K is a composite chemical equilibrium constant, consisting of a Henry's law solubility constant and equilibrium constants for the dissociation of carbonic acid into bicarbonate and the dissociation of bicarbonate into carbonate. As long as $[HCO_3^-] \gg [CO_3^{2-}]$, $K \times pCO_2$ and $[CO_3^{2-}]$ are approximately inversely related which suggests that $K \times pCO_2 \propto [CO_3^{2-}]^{-1}$. Or slightly more accurately:

$$K \times pCO_2 \propto [CO_3^{2-}]^{-O} \quad (4)$$

where we have used the quantity O, defined by *Omta et al.* [2010]:

$$O \equiv -\frac{\partial \ln(K \times pCO_2)}{\partial \ln([CO_3^{2-}])} \quad (5)$$

Under constant alkalinity, O is given by:

$$O = 1 + 4 \times \frac{[CO_3^{2-}]}{[HCO_3^-]} \approx 1.4 \quad (6)$$

O provides a useful conceptual tool because:

[8] 1. O is almost constant. $\frac{[CO_3^{2-}]}{[HCO_3^-]}$ is small (only about 0.1) which means that O varies between 1.2 and 1.6 at the surface of the world's oceans, considerably less than the commonly used Revelle buffer factor [*Bolin and Eriksson*, 1959] which varies between 8 and 15 [*Watson and Liss*, 1998].

[9] 2. The dependence of O on oceanic carbon and carbonate alkalinity is transparent, because it is a simple function of $[CO_3^{2-}]$ and $[HCO_3^-]$. O decreases monotonically with increasing DIC concentration: as CO_2 is added to the ocean, it reacts with CO_3^{2-} to form HCO_3^-, and therefore, the ratio $\frac{[CO_3^{2-}]}{[HCO_3^-]}$ decreases. Similarly, $\frac{[CO_3^{2-}]}{[HCO_3^-]}$ goes up with carbonate alkalinity, and therefore, O increases monotonically with increasing carbonate alkalinity.

2.1. Temperature Dependence of the Air-Sea Partitioning of Carbon

2.1.1. Air-Sea Carbon Partitioning: Analytical Derivation

[10] We now use the properties of O to derive the dependence of atmospheric pCO_2 on the water temperature averaged over the global ocean. The derivation is quite long, but the basic idea is relatively simple: we differentiate a global conservation equation for carbon with respect to temperature and collect the terms, so that we are left with an expression for $\frac{dpCO_2}{dT}$. Throughout the derivation, different parameters are introduced, the value ranges of which are given in Table 1.

Table 2. Simulation Parameter Values

Parameter	Units	Value	Interpretation
V	L	$3.1*10^{20}$	Volume of the ocean
M	mol	$3.0*10^{19}$	Gas amount in the atmosphere
A	mM	2.3	Carbonate alkalinity

[11] We start by writing down the equation for the global conservation of carbon in the ocean-atmosphere system (as explained in more detail by *Ito and Follows* [2005]):

$$M \times pCO_2 + V \times C + \int C_{reg} dV = C_t \tag{7}$$

with M the total gas content of the atmosphere in mol, V the volume of the ocean, C the average preformed carbon concentration in the global ocean, C_{reg} the extra carbon in the deep ocean that is a consequence of remineralisation/redissolution of organic material, and C_t the total carbon content of the ocean-atmosphere system. We assume that carbon at the ocean surface is equilibrated with the atmosphere which means that we can neglect the disequilibrium contribution to total DIC. Using the definitions for C and A, we can rewrite equation (7) as:

$$M \times pCO_2 + V \times \left(A - \left[CO_3^{2-}\right] + [CO_2]\right) = C_t - \int C_{reg} dV \tag{8}$$

with A the average preformed carbonate alkalinity in the ocean.

[12] Next, we differentiate equation (8) with respect to T, assuming that A, C_t, and C_{reg} are constant:

$$M \times \frac{dpCO_2}{dT} + V \times \left(-\frac{d\left[CO_3^{2-}\right]}{dT} + \frac{d[CO_2]}{dT}\right) = 0 \tag{9}$$

$[CO_3^{2-}]$ depends on T 'directly', i.e., because the carbonate system depends on temperature, and 'indirectly', because $[CO_3^{2-}]$ depends on pCO_2 which in turn depends on temperature. We need to take both effects into account when determining $\frac{d\left[CO_3^{2-}\right]}{dT}$:

$$\frac{d\left[CO_3^{2-}\right]}{dT} = \frac{\partial\left[CO_3^{2-}\right]}{\partial T} + \frac{\partial\left[CO_3^{2-}\right]}{\partial pCO_2} \times \frac{dpCO_2}{dT} \tag{10}$$

From the definition of O (equation 5), it can be shown that when pCO_2 is kept constant

$$\frac{\partial\left[CO_3^{2-}\right]}{\partial T} = \frac{\left[CO_3^{2-}\right] \times a}{O} \tag{11}$$

The parameter $a \equiv -\frac{\partial \ln K}{\partial T}$ (calculated from *Mehrbach et al.* [1973] and *Millero* [1995]) decreases from $0.052°C^{-1}$ at 0°C to $0.041°C^{-1}$ at 30°C. Furthermore,

$$\frac{\partial\left[CO_3^{2-}\right]}{\partial pCO_2} = -\frac{\left[CO_3^{2-}\right]}{O \times pCO_2} \tag{12}$$

which yields

$$\frac{d\left[CO_3^{2-}\right]}{dT} = \frac{\left[CO_3^{2-}\right]}{O} \times \left(a - \frac{1}{pCO_2}\frac{dpCO_2}{dT}\right) \tag{13}$$

The solubility of CO_2 in water follows Henry's law:

$$pCO_2 = K_H \times [CO_2] \tag{14}$$

with K_H a Henry's law constant. Analogous with equation (13), we obtain:

$$\frac{d[CO_2]}{dT} = \frac{\partial[CO_2]}{\partial T} + \frac{\partial[CO_2]}{\partial pCO_2} \times \frac{dpCO_2}{dT} = [CO_2] \times \left(-b + \frac{1}{pCO_2} \times \frac{dpCO_2}{dT}\right) \tag{15}$$

with the parameter $b \equiv \frac{\partial \ln K_H}{\partial T}$ decreasing from $0.039°C^{-1}$ at 0°C to $0.023°C^{-1}$ at 30°C, according to *Millero* [1995]. Using (13) and (15), we can rewrite equation (9) as:

$$M \times \frac{dpCO_2}{dT} + V \times \left(\frac{\left[CO_3^{2-}\right]}{O} \times \left(-a + \frac{1}{pCO_2} \times \frac{dpCO_2}{dT}\right) + [CO_2] \times \left(-b + \frac{1}{pCO_2} \times \frac{dpCO_2}{dT}\right)\right) = 0 \tag{16}$$

Collecting all the terms with $\frac{dpCO_2}{dT}$ on the left-hand side yields:

$$\frac{dpCO_2}{dT} \times \left(M + \frac{V}{pCO_2} \times \left(\frac{\left[CO_3^{2-}\right]}{O} + [CO_2]\right)\right) = V \times \left(\frac{\left[CO_3^{2-}\right] \times a}{O} + b \times [CO_2]\right) \tag{17}$$

and with $f \equiv \frac{M \times pCO_2 \times O}{\left[CO_3^{2-}\right] \times V} + \frac{O \times [CO_2]}{\left[CO_3^{2-}\right]}$:

$$\frac{dpCO_2}{dT} = \frac{\left(a + \frac{b \times O \times [CO_2]}{\left[CO_3^{2-}\right]}\right) \times pCO_2}{1 + f} \tag{18}$$

which we can simplify to:

$$\frac{dpCO_2}{dT} = \frac{pCO_2}{T_B} \tag{19}$$

where $T_B \equiv \frac{f+1}{a + \frac{b \times O \times [CO_2]}{\left[CO_3^{2-}\right]}}$. Although it appears to be a rather complex quantity, T_B actually remains approximately constant when the ocean temperature changes, because:

[13] 1. f remains approximately constant. A temperature increase leads to an increase in pCO_2 which tends to increase f, but also to an increase of $[CO_3^{2-}]$ which tends to decrease f. Furthermore, with pCO_2 = 280 ppmv, $[CO_3^{2-}]$ = 0.2 mM, O = 1.4, K_H = 27 L atm/mol and values for M and V from Table 2, f is only about 0.3, so small variations in f will not have a strong impact on the term $1 + f$.

[14] 2. Variations in a are relatively modest: a decreases from $0.052°C^{-1}$ at 0°C to $0.041°C^{-1}$ at 30°C; variations in

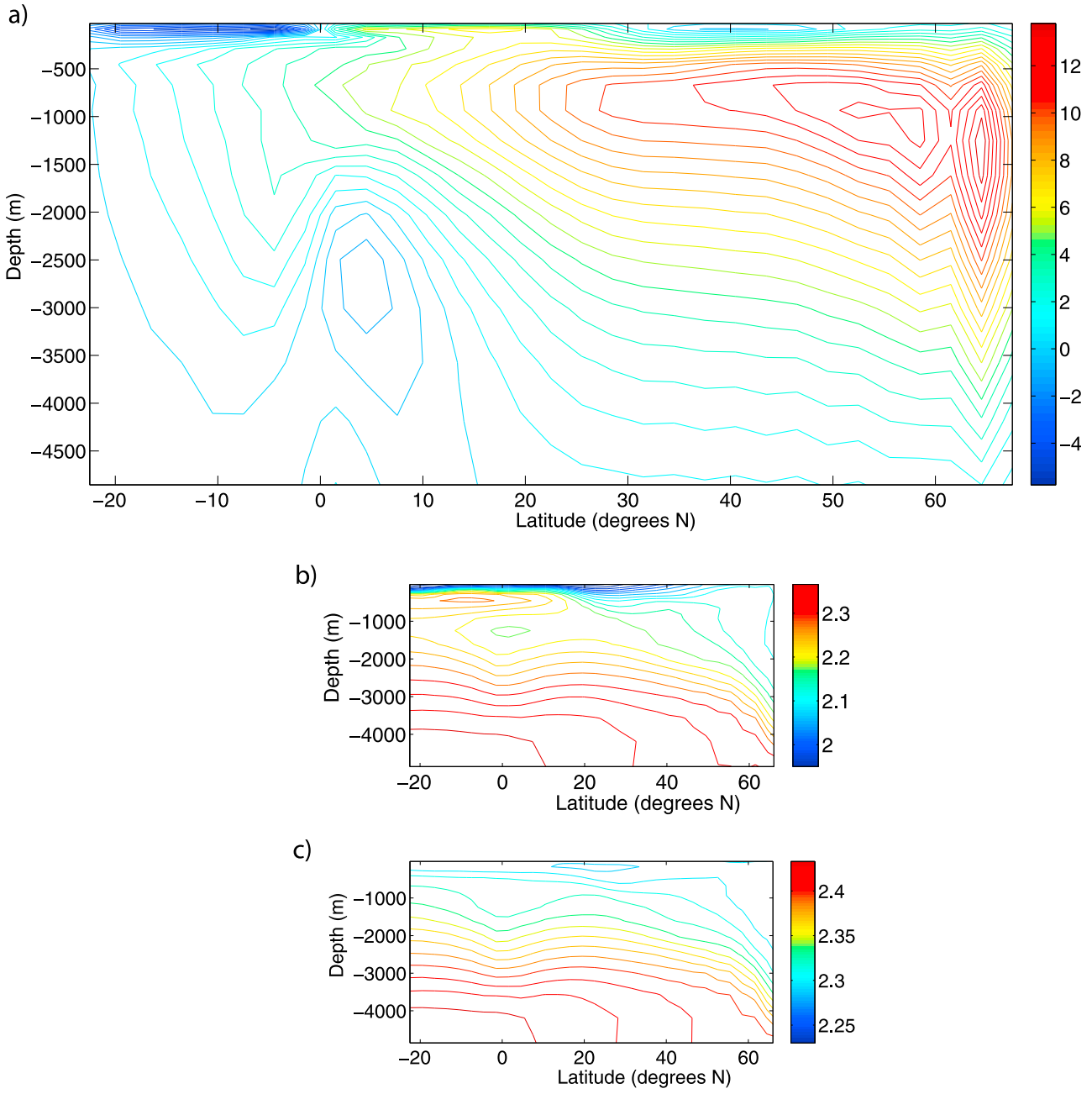

Figure 1. (a) Simulated Meridional Overturning Circulation stream function (Sv), (b) distributions along a transect through the middle of the basin of DIC (mM), and (c) total titration alkalinity (mM) after 20,000 years of spinup without biogeochemistry and 20,000 years with biogeochemistry included as a function of latitude (°N) and depth (m) at an average ocean temperature of 2.7°C.

the term $\frac{b\times O\times[CO_2]}{[CO_3^{2-}]}$ have little impact, as this term is only about $0.002°C^{-1}$.

[15] Since T_B is to a first approximation independent of T, equation (19) suggests an exponential dependence of atmospheric pCO_2 on the temperature of the ocean. With the parameters from Table 1, $T_B \approx 27°C$ which means that an increase in the ocean temperature of 1°C leads to an increase in atmospheric pCO_2 of about 4%. Thus, a very simple equation relates global ocean temperature and atmospheric pCO_2, with a single parameter, quantifiable from basic knowledge of the carbonate system. We will further analyze the validity of this relationship by comparing predicted values with actual ocean biogeochemistry simulation outputs.

2.1.2. Air-Sea Carbon Partitioning: Numerical Simulations

[16] To test the validity of relationship (19) between ocean temperature and atmospheric pCO_2 in a more realistic three-

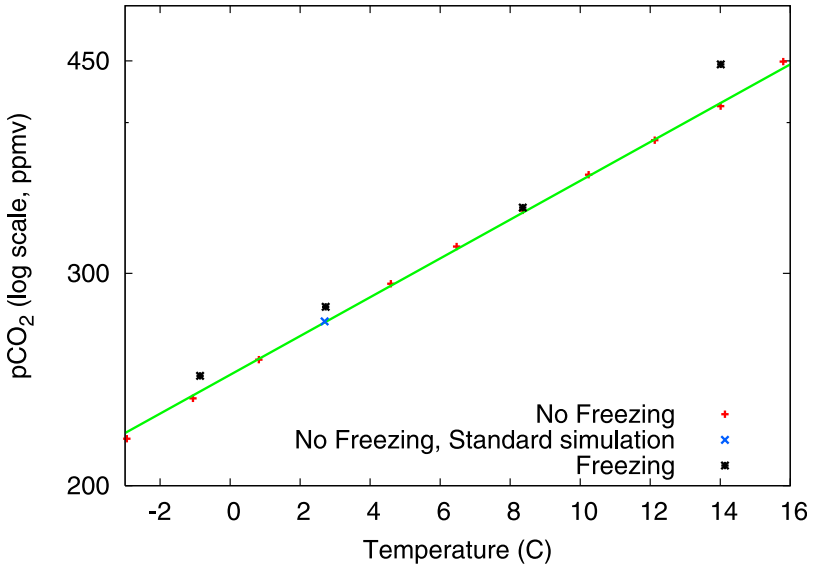

Figure 2. Comparison of simulation results with the theoretical prediction of pCO_2 (with pCO_2 in ppmv on a log scale) as a function of temperature (in °C). The standard simulation that should represent the preindustrial ocean (average temperature 2.7°C) is represented by a blue cross, and the other simulations with a linear equation of state and without freezing are indicated with red crosses. The black stars represent simulations with a nonlinear equation of state and with freezing. The green line gives the slope of $(27°C)^{-1}$ predicted from equation (19). This equation does not tell us where the intercept lies, and therefore, we used the first simulated point as intercept.

dimensional ocean-atmosphere system, we perform a set of experiments with a numerical ocean-atmosphere carbon cycle model using parameter values given in Table 2. Similar to *Follows et al.* [2002] and *Ito and Follows* [2003], we use the MIT ocean circulation model [*Marshall et al.*, 1997] configured in a sector extending from 24°S to 69° N, and sixty degrees wide at 3° × 3° horizontal resolution. There are fifteen levels from 50 m thick (uppermost) increasing downward to 690 m, with the ocean floor at 5000 m. Sea surface temperature is restored to monthly fields [*Levitus et al.*, 1994]. The biogeochemical cycles of carbon, phosphorus, oxygen and total titration alkalinity are coupled to the circulation model. The full carbonate chemistry is solved explicitly [*Follows et al.*, 2006] and the air-sea exchange of CO_2 is parameterized with a gas transfer coefficient assuming a constant uniform wind speed. A well-mixed atmospheric box is coupled to the ocean carbon cycle such that the partitioning of carbon between the atmosphere and the ocean is explicitly calculated; the model conserves total carbon. The atmospheric mixing ratio of CO_2 adjusts according to the net air-sea CO_2 flux at each time step. There is an explicit but idealized representation of the biological carbon pump following *Dutkiewicz et al.* [2005]. Further details about the model setup are given in Appendix A.

[17] In a suite of model experiments, we change the target to which sea surface temperature is being restored in steps of 2°C and reequilibrate the model, thus changing the global mean ocean temperature. We have chosen to investigate an (unrealistically) large range of global mean ocean temperatures to test the theoretical relationship (19). In general, the experiments are close to equilibrium with respect to the partitioning of carbon between the atmosphere and the ocean after 1000 years, but small drifts persist for over 10,000 years; for thoroughness we spun the physical model up for 20,000 years without the biogeochemical module and then for another 20,000 years with biogeochemistry. We maintain the latitudinal temperature gradients, the seasonality and, for simplicity, we do not allow freezing of the ocean water. The initial total titration alkalinity distribution is the same in each run.

[18] The overturning stream function and vertical distributions of DIC and total titration alkalinity for the 'standard' simulation at an average ocean temperature of 2.7°C are shown in Figure 1. The model reproduces the observed vertical gradients of DIC and total titration alkalinity [*Sarmiento and Gruber*, 2006]. The structure of the overturning circulation changes very little with altered global mean ocean temperature, because the meridional SST gradients are the same in all of the simulations and we do not allow for freezing. Because $T_B \approx 27°C$, the simulated values of $\ln(pCO_2)$ as a function of the average temperature of the ocean should lie on a straight line with a slope of $(27°C)^{-1}$. In Figure 2, we show such a slope, along with the simulated atmospheric pCO_2 plotted on a log scale as a function of the average temperature, integrated over the entire ocean. There is a very good agreement between the analytical theory and the simulations, even though many additional complexities of the ocean biogeochemistry are included in the numerical model (e.g., the impact of the biology and of temperature gradients in the ocean). We have also performed four simulations in which we allowed the seawater to freeze and

we used a nonlinear equation of state. As can be seen in Figure 2, these simulations show slightly less agreement with the analytical prediction, but the overall trend is well reproduced. A comparison with earlier simulations by *Goodwin and Lenton* [2009] and with observations of *Takahashi et al.* [1993] is provided in Appendix B.

2.2. Alkalinity Dependence

[19] On geologic timescales, neither the carbonate alkalinity nor the total titration alkalinity can be considered constant, as various alkaline salts are added to the ocean through rock weathering and the ocean loses alkalinity through carbonate sedimentation. We use the same framework to investigate the relationship between the ocean-atmosphere partitioning of carbon and ocean carbonate alkalinity. The details of the derivation are given in Appendix C, but the procedure is analogous to the derivation of the temperature dependence. We start from the global carbon conservation equation (8), take the derivative with respect to carbonate alkalinity, and collect the different terms in such a way that we find the derivative of pCO_2 with respect to carbonate alkalinity. The resulting relationship is:

$$\frac{dpCO_2}{dA} = \frac{-pCO_2 \times (O+1)}{2 \times \left[CO_3^{2-}\right] + 2 \times pCO_2 \times O\left(\frac{M}{V} + \frac{1}{K_H}\right)} \tag{20}$$

We can define $A_B \equiv \frac{2 \times O}{V \times (O+1)} \times \left(\frac{V \times \left[CO_3^{2-}\right]}{O} + pCO_2 \times \left(M + \frac{V}{K_H}\right)\right)$, such that:

$$\frac{dpCO_2}{dA} = \frac{-pCO_2}{A_B} \tag{21}$$

A_B is analogous to T_B and the factor I_B that was introduced by *Goodwin et al.* [2007, 2008] to describe the dependence of atmospheric pCO_2 on total carbon emissions (after full equilibration between the atmospheric and oceanic reservoirs). Since $I_B = \left(M + \frac{V}{K_H}\right) \times pCO_2 + V \times \frac{\left[CO_3^{2-}\right]}{O}$ [*Omta et al.*, 2010], there exists a relatively simple relationship between A_B and I_B: $A_B = \frac{2 \times I_B \times O}{V \times (O+1)}$.

[20] A_B consists of two terms, $\frac{V \times \left[CO_3^{2-}\right]}{O}$ and $pCO_2 \times \left(M + \frac{V}{K_H}\right)$; the relative sizes of these terms give rise to three different regimes (analogous to those given by *Omta et al.* [2010] when changing the carbon in the ocean-atmosphere system) in which it is possible to approximate equation (20) by simpler relationships:

[21] 1. High carbonate alkalinity: $\frac{V \times \left[CO_3^{2-}\right]}{O} \gg pCO_2 \times \left(M + \frac{V}{K_H}\right)$. For the ocean-atmosphere system, this is the case, if $A > 2.6$ mM. Though the average value of A at the ocean surface is about 2.2 mM, there are regions where A is much higher (e.g., in the Black Sea, surface carbonate alkalinity is around 3.2 mM [*Hiscock and Millero*, 2006]). In this regime, we cannot expect O to be constant, as $4 \times \frac{\left[CO_3^{2-}\right]}{\left[HCO_3^-\right]}$ is rather large. However, in the work of *Omta et al.* [2010], we defined the constant-alkalinity factor H:

$$H \equiv \frac{\partial \ln(K \times pCO_2)}{\partial \ln[H^+]} = 1 + 2 \times \frac{\left[CO_3^{2-}\right]}{A} \tag{22}$$

As long as $[CO_3^{2-}] \ll [HCO_3^-]$, H behaves qualitatively very similar to O: it is slightly above 1, approaching 1 as carbonate alkalinity decreases. However, if $[CO_3^{2-}] \gg [HCO_3^-]$, O approaches infinity, whereas H approaches 2; that is, H remains much more constant. Assuming that H is constant implies that $pCO_2 \propto [H^+]^H$. At equilibrium, $[H^+] = \frac{\left[HCO_3^-\right]}{K_2\left[CO_3^{2-}\right]}$ (with K_2 an equilibrium constant). Using $A \equiv [HCO_3^-] + 2 \times [CO_3^{2-}]$, we find that $[H^+] = \left(\frac{A}{\left[CO_3^{2-}\right]} - 2\right)/K_2$, from which we obtain:

$$pCO_2 \propto \left(\frac{A}{\left[CO_3^{2-}\right]} - 2\right)^H \tag{23}$$

Furthermore, if we neglect atmospheric carbon and oceanic carbon in the form of CO_2 (which are both very low in this regime) in the carbon conservation equation, then rearranging equation (8) leads to:

$$\left[CO_3^{2-}\right] \approx A + \frac{\int C_{reg} dV}{V} - \frac{C_t}{V} \tag{24}$$

Combining equations (23) and (24), we find

$$pCO_2 \propto \left(\frac{A}{A - \frac{C_t - \int C_{reg} dV}{V}} - 2\right)^H \tag{25}$$

Hence, pCO_2 appears to have a (rather complicated) power law dependence on carbonate alkalinity in this regime.

[22] 2. Intermediate regime: $\frac{V \times \left[CO_3^{2-}\right]}{O} \approx pCO_2 \times \left(M + \frac{V}{K_H}\right)$. With increasing alkalinity, $[CO_3^{2-}]$ goes up and pCO_2 goes down which makes A_B approximately constant. If A_B is constant, then the solution of equation (21) is an exponential relationship between pCO_2 and A:

$$pCO_2 \propto e^{-\frac{A}{A_B}} \tag{26}$$

Judging from Figure 4, this is the case for 1.9 mM $< A <$ 2.3 mM. Today's ocean is in this situation, as $A \approx 2.2$ mM.

[23] 3. Very low carbonate alkalinity: $\frac{V \times \left[CO_3^{2-}\right]}{O} \ll pCO_2 \times \left(M + \frac{V}{K_H}\right)$. This is the case, if $A < 1.8$ mM (e.g., in the Baltic Sea, $A \approx 1.5$ mM [*Hjalmarsson et al.*, 2008]). Since $O \approx 1$ in this regime, we can write

$$\frac{dpCO_2}{dA} \approx \frac{-1}{\frac{M}{V} + \frac{1}{K_H}} \tag{27}$$

which implies a linear relationship between pCO_2 and A.

[24] Similar to section 2.1.2, we have performed numerical simulations with the physical biogeochemical model to test relationship (21). In each of the simulations, we changed the global average total titration alkalinity by 0.1 mM when initializing the three-dimensional total titration alkalinity distribution, although we maintained the same latitudinal and vertical gradients. With $pCO_2 = 280$ ppmv, $[CO_3^{2-}] = 0.2$ mM and parameter values from Table 1, we expect that $A_B \approx 0.21$ mM. In Figure 4, we show the simulated $\ln(pCO_2)$ as a function of average ocean total titration alkalinity, along with a line with a slope corresponding to $A_B = 0.21$ mM. As can be seen, the

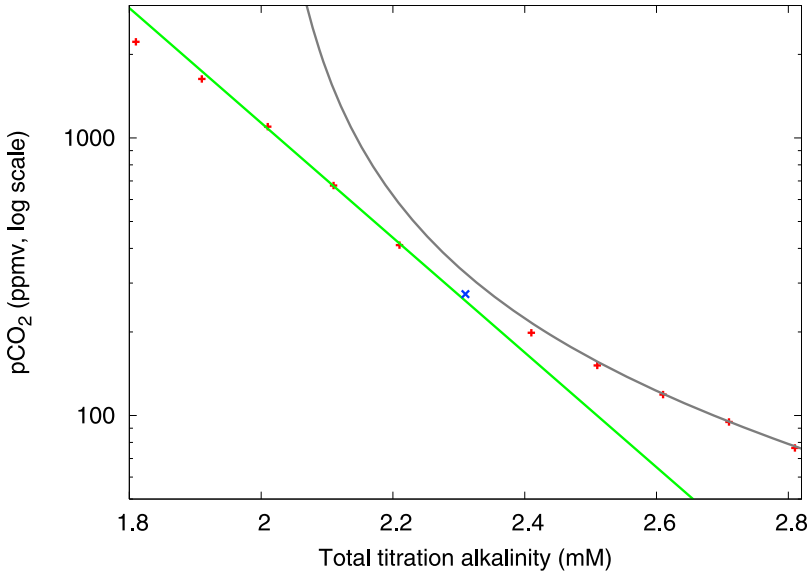

Figure 3. Comparison of simulation results with the theoretical prediction of pCO_2 (with pCO_2 in ppmv on a log scale) as a function of total titration alkalinity (in mM). The standard simulation that should represent the preindustrial ocean (average surface total titration alkalinity 2.3 mM) is represented by a blue cross, and the other simulations are indicated with red crosses. Part of the simulations is in the exponential regime, and another part falls in the power law region. The linear regime occurs at alkalinities lower than in our simulations. The green line indicates the exponential dependence with A_B at a constant value of 0.21 mM (equation (26)), whereas the grey line signifies the power law curve equation (25) where we have taken $\frac{C_t - \int C_{regdV}}{V}$ = 2.0 mM and H = 1.5.

simulations start to diverge from the straight line just above the current-day total titration alkalinity. This is the transition from an exponential to a power law type of dependence.

2.3. Comparison Between Analytical Predictions and Observations

2.3.1. Carbon Dioxide Variations at Constant DIC

[25] Concerned with seasonal variations in the fluxes of CO_2 across the air-sea interface, *Takahashi et al.* [1993] measured pCO_2 as a function of temperature in water samples each with the same DIC concentration. They found that $\frac{\partial \ln(pCO_2)}{\partial T} \approx 0.0423°C^{-1}$. To derive this relationship, we use that any 'direct' change in DIC as a consequence of a change in temperature must be offset by an 'indirect' change in DIC, resulting from a different pCO_2:

$$\frac{dC}{dT} = \frac{\partial C}{\partial T} + \frac{\partial C}{\partial \ln(pCO_2)} \frac{\partial \ln(pCO_2)}{\partial T} = 0 \qquad (28)$$

which leads to

$$\frac{\partial \ln(pCO_2)}{\partial T} = -\frac{\left(\frac{\partial C}{\partial T}\right)}{\left(\frac{\partial C}{\partial \ln(pCO_2)}\right)} = \frac{\frac{\left[CO_3^{2-}\right] \times a}{O} + b \times [CO_2]}{\frac{\left[CO_3^{2-}\right]}{O} + [CO_2]} \qquad (29)$$

With pCO_2 = 280 ppmv, $[CO_3^{2-}]$ = 0.2 mM and parameter values from Table 1, we find $\frac{\partial \ln(pCO_2)}{\partial T} \approx 0.045°C^{-1}$, slightly higher than observed by *Takahashi et al.* [1993]. It is worth noting that this value is close to $\frac{1}{T_B} \approx 0.037°C^{-1}$. Hence, if we had calculated T_B by simply assuming that the average oceanic preformed carbon concentration stays constant when the average temperature of the ocean changes, we would still have obtained a quite good estimate. The reason for this is that the oceanic carbon inventory is much larger than the atmospheric inventory: any change in the atmospheric pCO_2 corresponds with an almost negligible change in the oceanic DIC concentration.

2.3.2. Carbon Disequilibrium at the Ocean Surface

[26] The carbonate distribution at the ocean surface determines the preformed DIC and, in part, the strength of the solubility carbon pump. One important issue is how well the carbon system at the ocean surface is equilibrated with the atmosphere, particularly at high latitudes. The bottleneck in the equilibration of the system is the air-sea exchange of CO_2, taking place on a time scale of weeks, whereas the acid-base reactions within water equilibrate on a time scale of seconds [*Zeebe and Wolf-Gladrow*, 2001]. Therefore, the equilibrium theory can be applied to derive relationships between the concentrations of the dissolved carbon species, even if their concentrations are far from equilibrated with respect to atmospheric pCO_2. Equilibrium of the associated acid-base reactions implies:

$$[CO_2] = \frac{\left[HCO_3^-\right]^2 \times K_0 \times K_1}{\left[CO_3^{2-}\right] \times K_2} \qquad (30)$$

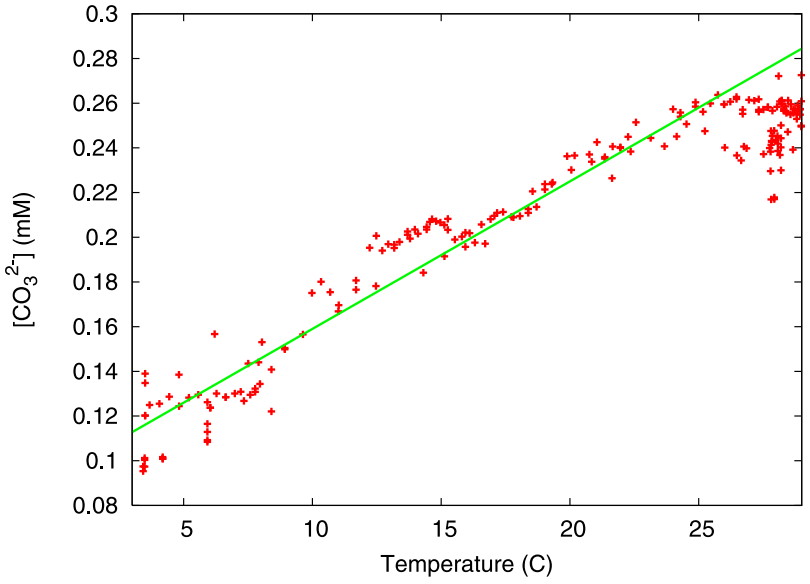

Figure 4. Comparison of theoretical prediction of carbonate concentration (in μM) as a function of annually averaged sea surface temperature (in °C) with observations. Data are taken from the World Ocean Atlas [*Loncarnini et al.*, 2006] (SST) and GLODAP [*Key et al.*, 2004] ($[CO_3^{2-}]$) along a meridional transect at 170°W. Observations are indicated with red crosses, and the green line indicates a constant slope of 6.6 $\mu M°C^{-1}$.

with K_0, K_1 and K_2 the respective reaction constants for the formation of carbonic acid from carbon dioxide and water, the dissociation of carbonic acid into bicarbonate, and the dissociation of bicarbonate into carbonate. This means that regardless of whether the oceanic and atmospheric carbon are at equilibrium, we have:

$$\frac{K_2 \times [CO_2]}{K_0 \times K_1} \propto \left[CO_3^{2-}\right]^{-O} \tag{31}$$

and therefore:

$$\frac{[CO_2]}{[CO_2]_{eq}} = \left(\frac{\left[CO_3^{2-}\right]}{\left[CO_3^{2-}\right]_{eq}}\right)^{-O} \tag{32}$$

with the subscript *eq* denoting the equilibrium concentration. This, for example, means that if $[CO_3^{2-}]$ is 8% above its equilibrium value, then $[CO_2]$ is about 10% below equilibrium. Thus, the extent to which $[CO_3^{2-}]$ is equilibrated at the ocean surface does provide a good measure of the equilibration of oceanic and atmospheric carbon.

[27] If the carbonate system is equilibrated with respect to atmospheric pCO_2 everywhere, then there should be a very simple relationship between $[CO_3^{2-}]$ at the ocean surface and the local (annually averaged) SST given by equation (11): $\frac{\partial\left[CO_3^{2-}\right]}{\partial T} = \frac{a \times \left[CO_3^{2-}\right]}{O} \approx 6.6\ \mu$ M/°C. This derivative is almost constant over a large range of temperatures, because $[CO_3^{2-}]$ and O increase and a decreases with increasing temperature. Thus, the theory predicts an approximately linear variation of $[CO_3^{2-}]$ with temperature. This relationship is observed in the surface ocean (using WOA and GLODAP: Figure 3), suggesting that the carbon system is indeed well equilibrated across the World Ocean.

3. Discussion and Conclusion

[28] We have derived analytical relationships for the air-sea partitioning of carbon as a function of ocean temperature and carbonate alkalinity. In general, the relative amount of carbon in the atmosphere with respect to the ocean increases with increasing ocean temperature and decreases with increasing carbonate alkalinity. The impact of temperature on the carbon partitioning generates a positive feedback: global warming resulting from the increasing amount of carbon in the atmosphere leads to a decreased oceanic carbon uptake which in turn increases the global warming. The relationship (19) between average ocean temperature and atmospheric pCO_2 suggests that this feedback is of moderate strength compared to the change in pCO_2 itself. For instance, an increase in the global average temperature by 3°C (which many models suggest with doubling of atmospheric pCO_2 [*Intergovernmental Panel on Climate Change*, 2007]) would lead to less carbon taken up by the oceans, eventually leading to around 10% higher atmospheric pCO_2.

[29] The theoretically predicted trend of atmospheric pCO_2 with temperature is consistent with numerical simulations of a more complex "ocean-like" system. In essence, the relationship is exponential because all the chemical equilibria involved (ocean-atmosphere partitioning of car-

bon dioxide as well as the chemical reactions that constitute the carbonate chemistry) have an Arrhenius-type (exponential) temperature dependence [*Weiss*, 1974]. However, the exponential relationship between ocean temperature and atmospheric pCO_2 will probably break down, once the composite factor $f \equiv \frac{M \times pCO_2 \times O}{[CO_3^{2-}] \times V} + \frac{O \times [CO_2]}{[CO_3^{2-}]}$ (see equation (18)) becomes larger than 1. This will be the case after high (anthropogenic) carbon emissions: for instance, at pCO_2 = 1000 ppmv and current alkalinity, $f \approx 2$.

[30] Throughout this article, we have assumed that the carbon system in the ocean is at equilibrium with atmospheric pCO_2. As was pointed out by *Toggweiler et al.* [2003], localized disequilibria can strongly impact atmospheric pCO_2. A compilation of results from various Ocean GCMs [*DeVries and Primeau*, 2009] suggests that the effect of disequilibria scales with the strength of the Atlantic Meridional Overturning Circulation, but that these effects are generally rather modest. Furthermore, the fact that the ocean-surface carbonate distribution as a function of temperature is predicted well by the theory (Figure 3) indicates that the carbonate system at the ocean surface is well-equilibrated with the atmospheric pCO_2.

[31] Between our experiments, the biological parametrization does not change. Changes in the biology can affect atmospheric pCO_2 primarily by impacting the ratio of preformed to remineralized nutrients [*Ito and Follows*, 2005]. Again, such effects are correlated with the strength of the Overturning Circulation, but they appear relatively modest [*Schmittner et al.*, 2007].

[32] The different regimes that emerge when carbonate alkalinity is changed are strikingly similar to the regimes that were identified under changing total carbon [*Omta et al.*, 2010]. Both carbonate alkalinity and total carbon affect the ocean *pH*: it increases with increasing carbonate alkalinity and decreasing total carbon. However, the power law regime seems much more relevant under varying carbonate alkalinity than under varying carbon. In fact, the theory and the simulations suggest that the current ocean with $A \approx 2.3$ mM is right at the edge of the exponential regime, near the transition to the power law regime. The anthropogenic carbon emissions will initially push the system into the exponential regime, but higher alkalinities due to increased weathering and deep-ocean carbonate dissolution may direct the ocean into the power law regime on longer timescales. Such a switch into power law behavior will imply that the more alkalinity is added to the system, the less impact further additions of alkalinity will have on atmospheric pCO_2.

[33] In this study, we have extended the theoretical framework that we introduced earlier [*Omta et al.*, 2010] to include the effects of temperature and carbonate alkalinity on atmospheric carbon. In general, we believe that this framework will be helpful to obtain a deeper insight into the ocean carbon system. Specifically, it could be applied to quantify the impact of ocean temperature and alkalinity on the radiative forcing resulting from atmospheric carbon in a way analogous to the *Goodwin et al.* [2009] relationship between the radiative forcing and changes in the atmosphere-ocean carbon inventory. Moreover, the framework could be used to analyze the carbon partitioning in climate change sensitivity studies [e.g., *Sokolov et al.*, 2009] and paleoclimatology simulations.

Appendix A: Detailed Description of the Model Setup

[34] The model density distribution is entirely determined by temperature using a linear equation of state; salinity is constant. Sea surface temperature is restored to monthly fields. In the control run, these fields are based on Atlantic Ocean climatological zonal means [*Levitus et al.*, 1994]. Similarly, the wind stress field is the zonal mean across the Atlantic taken from *Trenberth et al.* [1989]. The large-scale effects of mesoscale eddy transfers are parameterized following *Gent and McWilliams* [1990] and a globally uniform background vertical mixing rate of 5×10^{-5} m^2/s is imposed for tracers (salt, temperature and biogeochemical). There is no explicit mixed-layer parametrization, but convective adjustment occurs when the water column is statically unstable.

[35] Initial fields of the tracers are given as depth-dependent mean values for the Atlantic from GLODAP [*Key et al.*, 2004] and the World Ocean Atlas [*Loncarnini et al.*, 2006]. A crude representation of the biological pump is included to maintain a gradient in inorganic carbon from surface to deep and a reasonable latitudinal surface distribution of DIC. Community production in the euphotic layer is based on the availability of light and macronutrients as in the works of *Dutkiewicz et al.* [2005], *Goodwin et al.* [2007], and *McKinley et al.* [2004]. Two thirds of net production are assumed to enter a semilabile dissolved organic pool which has a remineralization time scale of 6 months; the remaining fraction of organic production is exported to depth as sinking particles where it is remineralized according to an empirical power law [*Martin et al.*, 1987]. Transformations of carbon and oxygen to and from the organic form are linked to those of phosphorus assuming fixed Redfield stoichiometry; the calcium carbonate cycle is parameterized using a fixed rain ratio.

Appendix B: Comparison Between Analytical Predictions and Goodwin and Lenton Simulation Results

[36] To obtain insight into the impact of temperature on the ocean carbon system, *Goodwin and Lenton* [2009] used the scheme proposed by *Follows et al.* [2006] to calculate numerically that $\frac{\partial C}{\partial T} \approx 0.10$ g/m^3 per °C, with pCO_2 held constant. Using our framework, an analytical expression for $\frac{\partial C}{\partial T}$ can be derived in a straightforward fashion:

$$\frac{\partial C}{\partial T} = -\frac{\partial [CO_3^{2-}]}{\partial T} + \frac{\partial [CO_2]}{\partial T} = -\frac{[CO_3^{2-}] \times a}{O} - b \times [CO_2] \tag{B1}$$

With pCO_2 = 280 ppm, $[CO_3^{2-}]$ = 0.2 mM, and parameter values as in Table 1, we find that $\frac{\partial C}{\partial T} \approx -0.007$ mol m^{-3}°C^{-1} which translates into a decrease of the (saturated) surface DIC of 0.08 g/m^3 per °C which is slightly lower than sug-

gested by *Goodwin and Lenton* [2009]. Since $\frac{[CO_3^{2-}]\times a}{O} \gg b \times [CO_2]$, the main reason for this decrease of DIC with increasing temperature is the fact that $[CO_3^{2-}]$ increases with increasing temperature.

[37] Goodwin and Lenton also investigated how $\frac{\partial C}{\partial T}$ changes as a function of atmospheric carbon content: their calculations suggest that $\frac{\partial\left(\frac{\partial C}{\partial T}\right)}{\partial \ln(pCO_2)} \approx 0.03$ g/m^3 per °C [see *Goodwin and Lenton*, 2009, Figure 2b]. Differentiating equation (B1) with respect to $\ln(pCO_2)$ (assuming O constant), we obtain:

$$\frac{\partial\left(\frac{\partial C}{\partial T}\right)}{\partial \ln(pCO_2)} = \frac{[CO_3^{2-}] \times a}{O^2} - b \times [CO_2] \tag{B2}$$

Filling in the numbers, we find $\frac{\partial\left(\frac{\partial C}{\partial T}\right)}{\partial \ln(pCO_2)} \approx 0.05$ g/m^3 per °C, considerably higher than reported by Goodwin and Lenton. Here, the decrease of $[CO_3^{2-}]$ with increasing pCO_2 turns out to be responsible for the fact that $\frac{\partial C}{\partial T}$ increases with increasing pCO_2.

Appendix C: Alkalinity Dependence Derivation

[38] To derive the dependence of pCO_2 on ocean carbonate alkalinity, we differentiate equation (7) with respect to A:

$$\frac{dpCO_2}{dA} + \frac{V}{M} \times \left(1 - \frac{d[CO_3^{2-}]}{dA} + \frac{d[CO_2]}{dA}\right) = 0 \tag{C1}$$

Because $[CO_2]$ obeys Henry's law, we simply have: $\frac{d[CO_2]}{dA} = \frac{1}{K_H e^{b\times\left(T-T_{ref}\right)}} \times \frac{dpCO_2}{dA}$, with K_H the Henry's law constant. For $\frac{d[CO_3^{2-}]}{dA}$, we get:

$$\frac{d[CO_3^{2-}]}{dA} = \frac{\partial[CO_3^{2-}]}{\partial A} + \frac{\partial[CO_3^{2-}]}{\partial pCO_2} \times \frac{dpCO_2}{dA} \tag{C2}$$

To find an explicit expression for $\frac{\partial[CO_3^{2-}]}{\partial A}$, we use the relationship between atmospheric pCO_2, $[HCO_3^-]$, and $[CO_3^{2-}]$ [*Broecker and Peng*, 1982]:

$$pCO_2 = \frac{[HCO_3^-]^2}{K \times [CO_3^{2-}]} = \frac{\left(A - 2 \times [CO_3^{2-}]\right)^2}{K \times [CO_3^{2-}]} \tag{C3}$$

Solving equation (C3) for $[CO_3^{2-}]$, we obtain:

$$[CO_3^{2-}] = \frac{A}{2} + \frac{K \times pCO_2}{8} \times \left(1 - \sqrt{\frac{8 \times A}{K \times pCO_2} + 1}\right) \tag{C4}$$

By differentiating the above equation, we get:

$$\frac{\partial[CO_3^{2-}]}{\partial A} = \frac{1}{2} \times \left(1 - \frac{1}{\sqrt{\frac{8\times A}{K\times pCO_2} + 1}}\right) \tag{C5}$$

and filling in the right-hand side of relationship (3) for pCO_2, we obtain:

$$\begin{aligned}\frac{\partial[CO_3^{2-}]}{\partial A} &= \frac{1}{2} \times \left(1 - \frac{[HCO_3^-]}{[HCO_3^-] + 4 \times [CO_3^{2-}]}\right) \\ &= \frac{1}{2} \times \left(1 - \frac{1}{O}\right).\end{aligned} \tag{C6}$$

[39] Combining equations (C2) and (C6), we find:

$$\frac{d[CO_3^{2-}]}{dA} = \frac{1}{2} \times \left(1 - \frac{1}{O}\right) - \frac{[CO_3^{2-}]}{O \times pCO_2} \times \frac{dpCO_2}{dA} \tag{C7}$$

and thus:

$$\begin{aligned}\frac{dpCO_2}{dA} + \frac{V}{M} \times \Bigg(&\frac{1}{2} \times \left(1 + \frac{1}{O}\right) + \frac{[CO_3^{2-}]}{O \times pCO_2} \times \frac{dpCO_2}{dA} \\ &+ \frac{1}{K_H \times e^{b\times\left(T-T_{ref}\right)}} \times \frac{dpCO_2}{dA}\Bigg) = 0\end{aligned} \tag{C8}$$

which after some algebra leads to

$$\frac{dpCO_2}{dA} = \frac{-pCO_2 \times (O+1)}{2 \times [CO_3^{2-}] + 2 \times pCO_2 \times O \times \left(\frac{M}{V} + \frac{1}{K_H \times e^{b\times\left(T-T_{ref}\right)}}\right)}. \tag{C9}$$

[40] **Acknowledgments.** We would like to thank Jean-Michel Campin and David Ferreira for assistance with the MIT GCM, and David Ferreira and three anonymous reviewers for helpful discussions and comments. A.W.O. was financially supported through a Rubicon fellowship provided by the Netherlands Organisation for Scientific Research (NWO). S.D. and M.J.F. are grateful for support from NOAA.

References

Archer, D. E., H. Kheshgi, and E. Maier-Reimer (1997), Multiple timescales for neutralization of fossil fuel CO_2, *Geophys. Res. Lett.*, *24*, 405–408.

Bacastow, R. B. (1996), The effect of temperature change of the warm surface waters of the oceans on atmospheric CO_2, *Global Biogeochem. Cycles*, *10*, 319–334.

Bolin, B., and E. Eriksson (1959), Distribution of matter in the sea and the atmosphere, in *The Atmosphere and the Sea in Motion*, edited by B. Bolin, pp. 130–142, Rockefeller Inst. Press, New York.

Broecker, W. S., and T. H. Peng (1982), *Tracers in the Sea*, Lamont-Doherty Geol. Obs., Palisades, N. Y.

Broecker, W. S., J. Lynch-Stieglitz, D. Archer, M. Hoffmann, E. Maier-Reimer, O. Marchal, T. Stocker, and N. Gruber (1999), How strong is the Harvardton-Bear constraint?, *Global Biogeochem. Cycles*, *13*, 817–820.

Chester, R. (2000), *Marine Geochemistry*, 2nd ed., Blackwell, Oxford, U. K.

DeVries, T., and F. Primeau (2009), Atmospheric pCO_2 sensitivity to the solubility pump: Role of the low-latitude ocean, *Global Biogeochem. Cycles*, *23*, GB4020, doi:10.1029/2009GB003537.

Dutkiewicz, S., M. J. Follows, and P. Parekh (2005), Interactions of the iron and phosphorus cycles: A three-dimensional model study, *Global Biogeochem. Cycles*, *19*, GB1021, doi:10.1029/2004GB002342.

Follows, M. J., T. Ito, and J. Marotzke (2002), The wind-driven, subtropical gyres and the solubility pump of CO_2, *Global Biogeochem. Cycles*, *16*(4), 1113, doi:10.1029/2001GB001786.

Follows, M. J., T. Ito, and S. Dutkiewicz (2006), On the solution of the carbonate system in biogeochemistry models, *Ocean Modell.*, *12*, 290–301.

Friedlingstein, P., et al. (2006), Climate-carbon cycle feedback analysis: Results from the C^4 MIP model intercomparison, *J. Clim.*, *19*, 3337–3353.

Gent, P. R., and J. C. McWilliams (1990), Isopycnal mixing in ocean circulation models, *J. Phys. Oceanogr.*, *20*, 150–155.

Goodwin, P., and T. M. Lenton (2009), Quantifying the feedback between ocean heating and CO_2 solubility as an equivalent carbon emission, *Geophys. Res. Lett.*, *36*, L15609, doi:10.1029/2009GL039247.

Goodwin, P., R. G. Williams, M. J. Follows, and S. Dutkiewicz (2007), Ocean-atmosphere partitioning of anthropogenic carbon dioxide on centennial timescales, *Global Biogeochem. Cycles*, *21*, GB1014, doi:10.1029/2006GB002810.

Goodwin, P., M. J. Follows, and R. G. Williams (2008), Analytical relationships between atmospheric carbon dioxide, carbon emissions, and ocean processes, *Global Biogeochem. Cycles*, *22*, GB3030, doi:10.1029/2008GB003184.

Goodwin, P., R. G. Williams, A. Ridgwell, and M. J. Follows (2009), Climate sensitivity to the carbon cycle modulated by past and future changes in ocean chemistry, *Nat. Geosci.*, *2*, 145–150.

Hiscock, W. T., and F. J. Millero (2006), Alkalinity of the anoxic waters in the Western Black Sea, *Deep Sea Res. II*, *53*, 1787–1801.

Hjalmarsson, S., K. Wesslander, L. G. Anderson, A. Omstedt, M. Perttilä, and L. Mintrop (2008), Distribution, long-term development and mass balance calculation of total alkalinity in the Baltic Sea, *Cont. Shelf Res.*, *28*, 593–601.

Intergovernmental Panel on Climate Change (2007), *Climate Change 2007. The Physical Science Basis. Contribution of Working Group I to the Fourth Assessment Report of the Intergovernmental Panel on Climate Change*, edited by S. Solomon et al., 996 pp., Cambridge Univ. Press, Cambridge, U. K.

Ito, T., and M. J. Follows (2003), Upper ocean control on the solubility pump of CO_2, *J. Mar. Res.*, *61*, 465–489.

Ito, T., and M. J. Follows (2005), Preformed phosphate, soft-tissue pump and atmospheric CO_2, *J. Mar. Res.*, *63*, 813–839.

Key, R. M., et al. (2004), A global ocean carbon climatology: Results from global data analysis project (GLODAP), *Global Biogeochem. Cycles*, *18*, GB4031, doi:10.1029/2004GB002247.

Lee, K., and F. J. Millero (1995), Thermodynamic studies of the carbonate system in sea water, *Deep Sea Res. I*, *42*, 2035–2061.

Levitus, S., R. Burgett, and T. P. Boyer (1994), *World Ocean Atlas* 1994, vol. 3, NOAA, Washington, D. C.

Loncarnini, R. A., V. Mishonov, J. I. Antonov, T. P. Boyer, and H. E. Garcia (2006), *World Ocean Atlas* 2005, vol. 1, NOAA, Washington, D. C.

Marshall, J., A. Adcroft, C. Hill, L. Perelman, and C. Heisey (1997), A finite-volume, incompressible Navier-Stokes model for studies of the ocean on parallel computers, *J. Geophys. Res.*, *102*, 5753–5766.

Martin, J. H., G. A. Knauer, D. M. Karl, and W. W. Broenkow (1987), VERTEX: Carbon cycling in the northeast Pacific, *Deep Sea Res. A*, *34*, 267–285.

McKinley, G. A., M. J. Follows, and J. Marshall (2004), Mechanisms of air-sea CO_2 flux variability in the equatorial Pacific and the North Atlantic, *Global Biogeochem. Cycles*, *18*, GB2011, doi:10.1029/2003GB002179.

McKinley, G. A., et al. (2006), North Pacific carbon cycle response to climate variability on seasonal to decadal timescales, *J. Geophys. Res.*, *111*, C07S06, doi:10.1029/2005JC003173.

Mehrbach, C., C. H. Culberson, J. E. Hawley, and R. M. Pytkowicz (1973), Measurement of the apparent dissociation constants of carbonic acid in seawater at atmospheric pressure, *Limnol. Oceanogr.*, *18*, 897–907.

Millero, F. J. (1995), Thermodynamics of the carbon dioxide system in the oceans, *Geochim. Cosmochim. Acta*, *59*, 661–677.

Omta, A. W., P. Goodwin, and M. J. Follows (2010), Multiple regimes of air-sea carbon partitioning identified from constant-alkalinity buffer factors, *Global Biogeochem. Cycles*, *24*, GB3008, doi:10.1029/2009GB003726.

Orr, J. C., et al. (2001), Estimates of anthropogenic carbon uptake from four three-dimensional global ocean models, *Global Biogeochem. Cycles*, *15*, 43–60.

Plattner, G. K., F. Joos, T. F. Stocker, and O. Marchal (2001), Feedback mechanisms and sensitivities of ocean carbon uptake under global warming, *Tellus, Ser. B*, *53*, 564–592.

Sarmiento, J. L., and N. Gruber (2006), *Ocean Biogeochemical Dynamics*, Princeton Univ. Press, Princeton, N. J.

Schmittner, A., E. J. Brook, and J. Ahn (2007), Impact of the ocean's overturning circulation on atmospheric CO_2, in *Ocean Circulation: Mechanisms and Impacts*, edited by A. Schmittner, J. Chiang, and S. Hemming, pp. 315–334, AGU, Washington, D. C.

Sokolov, A. P., et al. (2009), Probabilistic forecast for twenty-first century climate based on uncertainties in emissions (without policy) and climate parameters, *J. Clim.*, *22*, 5175–5204.

Takahashi, T., J. Olafsson, J. G. Goddard, D. W. Chipman, and S. C. Sutherland (1993), Seasonal variation of CO_2 and nutrients in the high-latitude surface oceans: A comparative study, *Global Biogeochem. Cycles*, *7*, 843–878.

Toggweiler, J. R., A. Gnanadesikan, S. Carson, R. Murnane, and J. L. Sarmiento (2003), Representation of the carbon cycle in box models and GCMs: 1. Solubility pump, *Global Biogeochem. Cycles*, *17*(1), 1026, doi:10.1029/2001GB001401.

Trenberth, K. E., J. G. Olson, and W. G. Large (1989), *A Global Wind Stress Climatology Based on ECMWF Analyses*, NCAR Tech. Note, Boulder, Colo.

Watson, A. J., and P. S. Liss (1998), Marine biological controls on climate via the carbon and sulphur geochemical cycles, *Philos. Trans. R. Soc. London B*, *353*, 41–51.

Weiss, R. F. (1974), Carbon dioxide in sea water: The solubility of a non-ideal gas, *Mar. Chem.*, *2*, 203–215.

Zeebe, R. E., and D. A. Wolf-Gladrow (2001), *CO_2 in Seawater: Equilibrium, Kinetics, Isotopes*, Elsevier, Amsterdam.

S. Dutkiewicz, M. J. Follows, and A. W. Omta, Department of Earth, Atmospheric and Planetary Sciences, Massachusetts Institute of Technology, 77 Massachusetts Ave., Cambridge, MA 02139, USA. (omta@mit.edu)